Journal of Microscopy, Vol. 239, Pt 2 2010, pp. 167–172
Received 22 July 2009; accepted 21 December 2009
doi: 10.1111/j.1365-2818.2010.03368.x

Leakage radiation microscopy of surface plasmon coupled emission: investigation of gain-assisted propagation in an integrated plasmonic waveguide

J. GRANDIDIER, G. COLAS DES FRANCS, S. MASSENOT, A. BOUHELIER, L. MARKEY, J.-C. WEEBER & A. DEREUX
Institut Carnot de Bourgogne, UMR 5209 CNRS - Université de Bourgogne, Dijon, France

Key words. Leakage radiation microscopy, plasmon, spaser, surface plasmon coupled emission.

Summary

Using a single-mode dielectric-loaded surface plasmon polariton waveguide doped with quantum dots, we were able to slightly increase the propagation length of the mode by stimulated emission of plasmon. We analyse the amplification phenomenon in the visible range by combining leakage radiation microscopy and surface plasmon coupled emission techniques.

Introduction

Metallic wires enable transmission of both electrical and optical (plasmonic) signals in the same circuitry, and are therefore of great interest for integrated electro-optics applications (Ozbay, 2006; Ebbesen *et al.*, 2008). The free electrons of a metal support eigenmodes, so-called surface plasmon polaritons (SPPs), resulting from the coupling of electrons gas coherent oscillations ('plasma quasi-particle') to photons ('polaritons' because they originate from matter polarization). Recently, the concept of dielectric–loaded surface plasmon polariton waveguide (DLSPPW) has been introduced (Steinberger *et al.*, 2006; Holmgaard & Bozhevolnyi, 2007; Krasavin & Zayats, 2008), directly inspired from standard integrated photonic configuration (Hunsperger, 2002). In this configuration, a dielectric strip above a metal film is associating in a single shot both the dielectric and metallic potentialities integrated on a surface. When optimized, a DLSPPW supports a mode efficiently confined into the dielectric strip with its maximum intensity located at the metal interface (Grandidier *et al.*, 2008). Active and dynamic control over the SPP mode (switching, modulation, nonlinear, ...) can then be performed. In this context, it was suggested that surface plasmon amplication by stimulated emission of radiation could occur, in strong analogy with laser phenomenon so that optical gain could compensate plasmon losses (Bergman & Stockman, 2003). In this paper, we analyse the influence of quantum dots (QDs) doping the dielectric strip on the DLSPPW mode. Under optical pumping, the QDs-doped strip acts as a gain medium. In a direct analogy to an optical amplifier, gain-assisted propagation in the integrated plamonic waveguide can be achieved (Grandidier *et al.*, 2009). This property is highly valuable in this context because a strong confinement of the mode in a DLSPPW is associated with an increase of losses jeopardizing thus applications of a fully integrated plasmonic circuitry.

In this communication, we experimentally investigate an optically assisted increase of the SPP propagation length by combining leakage radiation microscopy (Drezet *et al.*, 2008; Grandidier *et al.*, 2008) and surface plasmon coupled emission (Gryczynski *et al.*, 2004, 2005a,b). QDs, and more generally fluorophores emitters, are point-like dipolar sources. The large wave spectrum of the emitted photons can couple in the available modes present in a waveguiding structure. For structures integrating thin metal films, plasmon modes are generally leaky so that they can be fully characterized by leakage radiation microscopy, in both direct and reciprocal (Fourier) spaces (Massenot *et al.*, 2007). In this work, we profit of the two abovementioned properties to extensively investigate modal properties of doped DLSPPW. In particular, we measured the number of supported modes as well as their effective indices and propagation lengths (Section 'Leakage Radiation Microscopy of Surface Plasmon Coupled Emission'). Section 'Mode Propagation and Losses Compensation' is devoted to the analysis of optical gain occurring during mode propagation within a DLSPPW.

Correspondence to: J. Grandidier, Institut Carnot de Bourgogne, UMR 5209 CNRS - Université de Bourgogne, 9 Av. A. Savary, BP 47 870, 21078 Dijon, France. Tel: +33(0)3 80 39 60 20; fax: +33(0)3 80 39 60 24; e-mail: jonathan.grandidier@u-bourgogne.fr

Leakage radiation microscopy of surface plasmon coupled emission

Film and multimode waveguide

As a reference experiment, we demonstrate the coupling properties between QD fluorescence and a surface plasmon mode in a two-dimensional configuration (films). We spin-coated a 78-nm PMMA film, doped with CdSe/ZnS core-shell nanocrystals (Evident Technologies) on a thin silver film (50 nm) thermally deposited on a glass cover slip. These quantum dots were chosen due to their high stability and strong absorption and emission cross-sections around $\lambda_{abs} = 530\,nm$ and $\lambda_{exc} = 620\,nm$, respectively. Figure 1 describes the principle of leakage radiation microscopy of surface plasmon coupled emission. A $\lambda = 532$ nm laser excites the Ag/QD-PMMA layer through a high numerical aperture (NA = 1.49) objective. As a result of the large spread of incident wave-vectors provided by the objective and the dipolar nature of the QDs emission, SPPs modes at the excitation wavelength and at the emission wavelengths are excited. These modes are leaky and give rise to spectrally resolvable radiation into the glass substrate. This situation is depicted in Fig. 2(a). QDs emission around $\lambda = 620$ nm is detected after filtering the reflected 532 nm illumination by a dichroic mirror. Figures 2(b) and (c) show true-colour photographs of the momentum distribution of the reflected pump light wavelength and of the QDs emission.

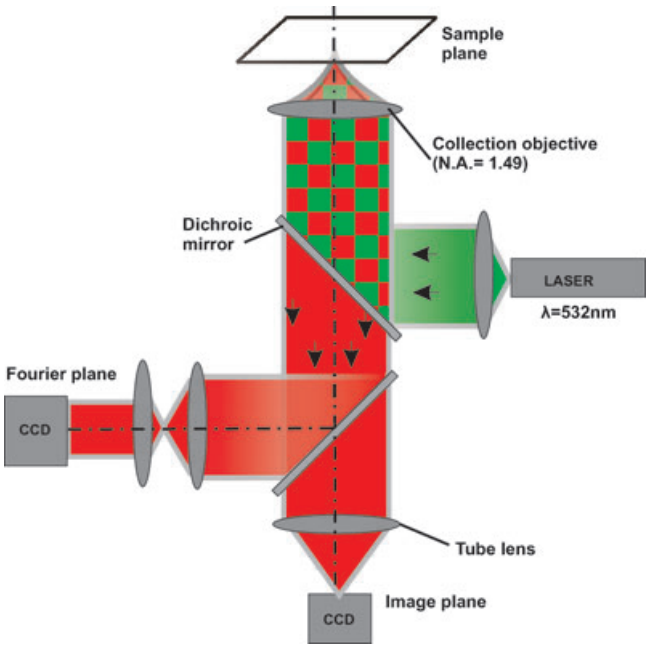

Fig. 1. Leakage radiation microscopy of surface plasmon coupled emission (LRM-SPCE) setup. The sample is locally excited at $\lambda = 532$ nm to pump the QDs. The leaky modes excited by the QDs emission are analysed in both Fourier and image planes. The dichroic mirror stops the reflected $\lambda = 532$ nm light used to optically pump the QDs.

The photographs were taken at the Fourier plane of the microscope without and with the dichroic mirror, respectively. The presence of an annular angular distribution of the emission (red) wavelength indicates that the QD fluorescence is coupled to an SPP mode. Because the QDs have an isotropic orientation of their emission moments in the polymer film, the SPP is isotropically excited at the metal/polymer interface as shown by the full circle. Importantly, the coupling of QDs emission to the surface plasmon mode also leads to emission quenching due to absorption in the metal (Enderlein & Ruckstuhl, 2005; Hoogenboom *et al.*, 2009). However, we use here a thin silver film limiting therefore this phenomenon.

We now investigate a doped-PMMA DLSPPW deposited on a silver film (Fig. 3a). The DLSPPW were produced by standard optical lithography and lift-off technique. The width and height of the doped polymer waveguide were fixed at 1.5 μm and 78 nm, respectively. We numerically investigated the reflectivity map of the structure using the differential method (Massenot *et al.*, 2008) with a plane wave excitation at 633 nm, corresponding to the red laser used in the next section and close to the emission maximum of the QDs. Figure 3(b) shows the calculated map in terms of normalized wavenumbers k_i/k_o $(i = x, y)$, where $k_o = 2\pi/\lambda$ is the free-space wavenumber. In these reduced coordinates systems, it is simple to define the objective numerical aperture ($\sqrt{(k_x/k_o)^2 + (k_y/k_o)^2} = NA = 1.49$) and the critical angle θ_c into the substrate ($\sqrt{(k_x/k_o)^2 + (k_y/k_o)^2} = n\sin\theta_c = 1$). This is helpful to calibrate the Fourier plane independently of the considered wavelength.

A bright contrast in the map corresponds to a reduced reflectivity. The main features in Fig. 3(c) are a series of horizontal lines in the upper and lower part of the reflectivity map. Each horizontal line defines a constant wavector component k_y along the guide axis. This is the propagation constant of the guided mode (Massenot *et al.*, 2007). It is convenient to define equivalently the mode effective index $n_{eff} = k_y/k_o$. For the dimensions considered here, four modes are visible corresponding to TM_{00}, TM_{01} TM_{02} and TM_{03}, respectively. They all have an effective index above 1 and below NA = 1.49. This clearly indicates that they are leaky modes that radiate into the substrate.

Figure 3(c) shows the measured Fourier plane centered at the emission intensity of the QDs. This image was obtained by homogeneously illuminating a series of adjacent self-similar waveguides to enhance the signal-to-noise ratio on the recorded signal. The distance between waveguides was 10 μm. The unpolarized emission of QDs insures that all the waveguide leaky modes are scanned by this method. A series of modes are also visible in this experimental image. The main difference with the calculated map resides in the width of the effective indices. For the calculated reflectivity, the modes are well separated because of monochromatic excitation. For Fig. 3(c), however, the breadth of the fluorescence emission broadens the width of the modes. As a consequence, only three

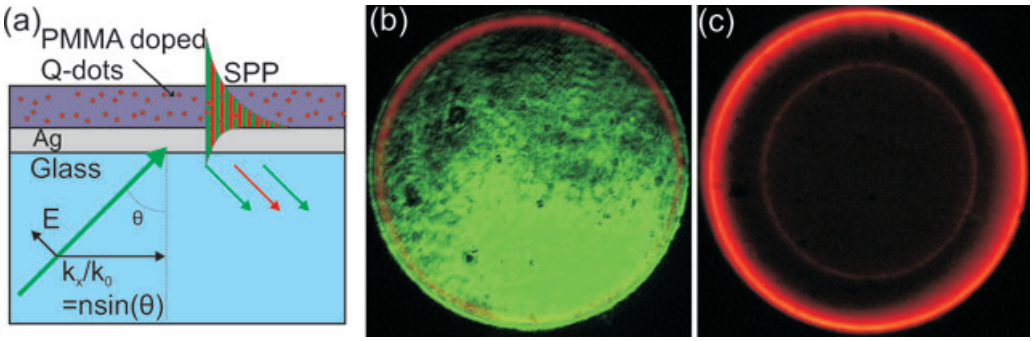

Fig. 2. (a) Schematic representation of green laser excitation of a QDs-doped PMMA film and detection of both green- and red-emitted SPP leakages in the substrate. (b–c) True colours photographs of the Fourier plane without (b) and with (c) the dichroic filter, respectively. In (b), the red circle superimposes to a depletion of the green incident field disk, demonstrating the absorption of green light to a $\lambda = 532$ nm SPP mode and red light QDs emission coupling to $\lambda \approx 620$ nm SPP mode.

modes are visible in the experimental image because the TM_{00} and TM_{01} seem to be degenerated.

The annular replica visible in the images (symmetric to the k_y/k_o axis) originate from diffraction orders because a periodic arrangement of waveguides were used both theoretically and experimentally. The differential method is adapted from grating theory so that it intrinsically concerns periodic structures. Because computation time strongly increases with the periodicity, a compromise has to be found for decoupling the property of a single structure with the property of an ensemble. In the calculation, we fixed the periodicity to $d = 8$ μm. The period in the reciprocal space follows $\delta = \lambda/d = 0.633/8 = 7.91 \times 10^{-2}$ in the calculated image (Fig. 3b). Similarly, the period of the replica measured in the experimental Fourier image is $\delta = \lambda/d \approx 0.620/10 = 6.2 \times 10^{-2}$ at the QDs emission peak (Fig. 3c).

Single-mode DLSPPW

Having fully assessed the availability of leakage radiation microscopy combined with surface plasmon coupled emission, we now investigate a single-mode QDs-doped DLSPPW. It consists of a 120-nm thick and 300-nm width structure. This waveguide has a single-mode operation because only one guided wave vector appears in the experimental Fourier plane shown in Fig. 4. We numerically determined the DLSPPW TM_{00} guided mode effective index 1.07 at $\lambda = 620$ nm in agreement the experimental one measured at $n_{\text{eff}} = 1.1$. The circle at $n_{\text{eff}} = k_y/k_o \approx 1$ originates from the Ag/air SPP mode excited at the QDs emission. The presence of this particular mode is at first surprising because the QDs are essentially located inside the polymer waveguide. However, we found that the lift off technique used to reveal the DLSPPW after lithography was never fully complete and patches of residues

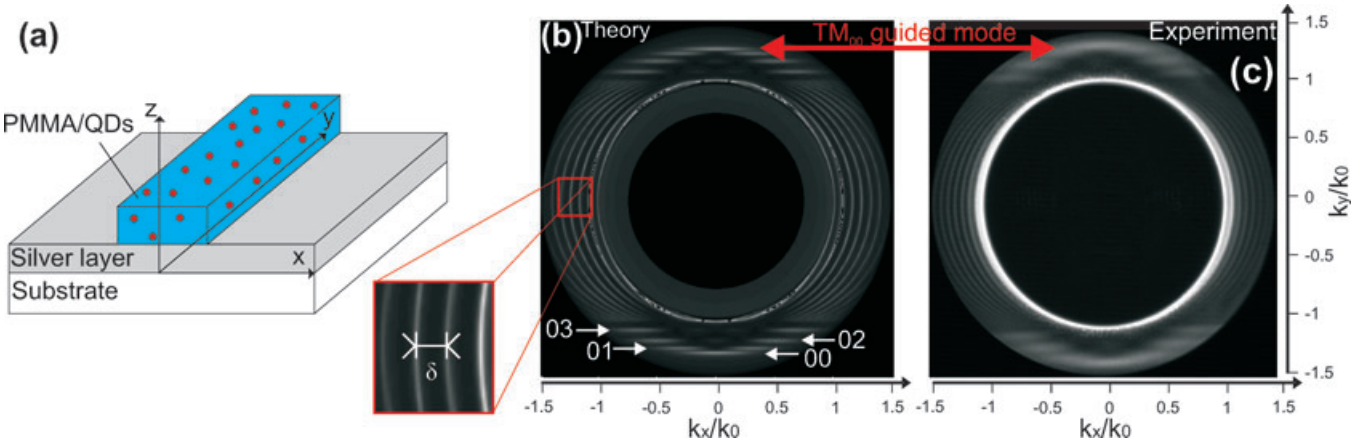

Fig. 3. (a) Schetch of the doped-DLSPPW (78 nm thick and 1.5 μm width). (b) Reflectivity calculated assuming a TM polarized incident plane wave ($\lambda = 633$ nm). The TM_{nm} modes orders (n,m) are indicated on the figure. The waveguide does not support any TE mode. The reflectivity is calculated between $k_i/k_o = 0.75$ and $k_i/k_o = 1.49$. (c) LRM image recorded in the Fourier plane around $\lambda = 620$ nm when the QDs-doped DLSPPW is excited from above with a defocused beam at $\lambda = 532$ nm (see also Fig. 5). Diffraction patterns perpendicular to waveguides axis have periodicities $\delta = 7.9 \times 10^{-2}$ and $\delta = 6.5 \times 10^{-2}$ in the calculated and measured images, respectively.

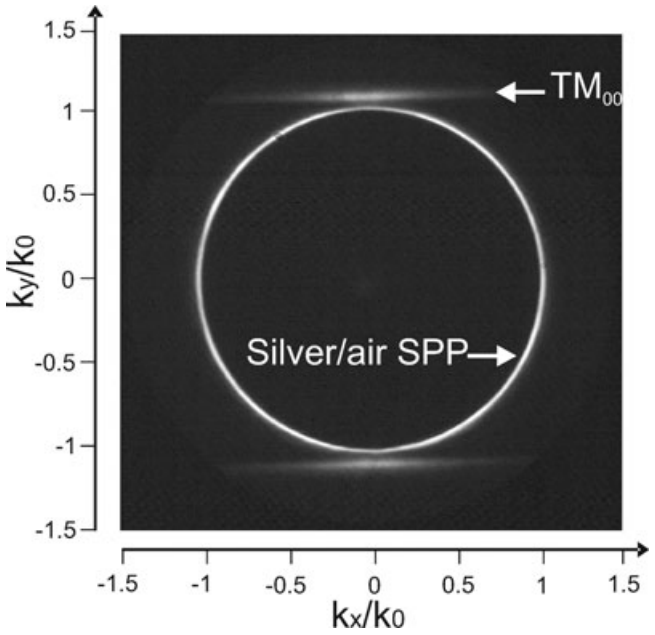

Fig. 4. LRM–SPCE image recorded in the Fourier plane around $\lambda = 620$ nm when a QDs-doped DLSPPW (120 nm thick and 300 nm width) is excited at $\lambda = 532$ nm. Horizontal line is the SPP TM_{00} waveguide mode leaking into the glass at $n_{\text{eff}} = k_y/k_o = 1.1$.

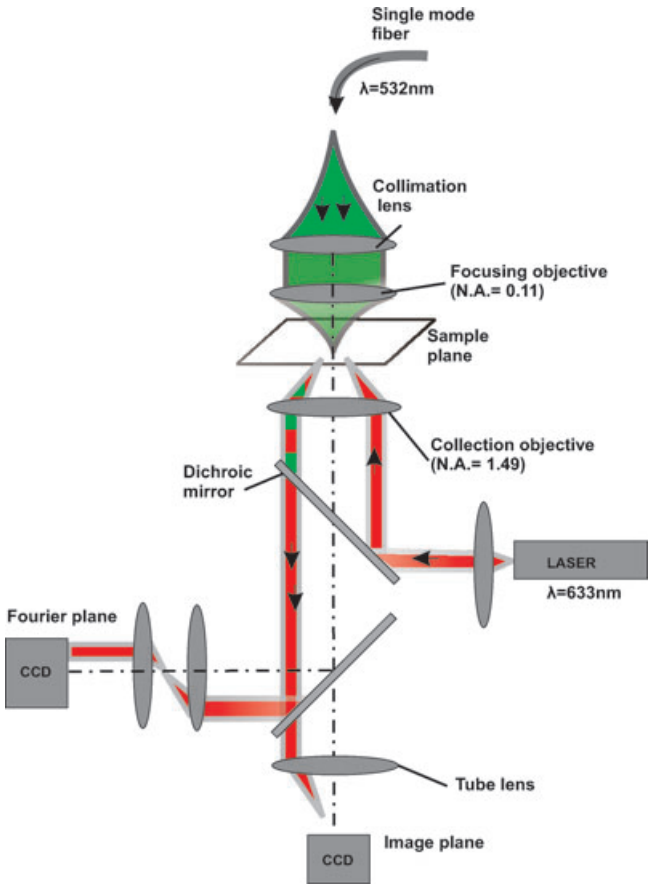

Fig. 5. Leakage radiation microscope setup. The QDs are homogeneously pumped in a diascopic configuration with defocused laser at $\lambda = 532$ nm. The DLSPPW mode at $\lambda = 633$ nm is resonantly excited episcopally by controlling the angle of incidence. Radiation leakages are analysed in both Fourier and image planes.

were always present on the Ag film in between the waveguides, giving rise to the abovementioned circle.

In the next section, we will investigate gain-assisted mode propagation in this single mode integrated plasmonic waveguide.

Mode propagation and losses compensation

In this last section, we focus on the propagation distance of the SPP in the single-mode waveguide (120 nm × 300 nm). To this purpose, we modify the setup of Fig. 1 to both launch a guided mode (direct excitation) and to optically pump the QDs. Figure 5 briefly represents the setup. The DLSPPW is first excited from the bottom at $\lambda = 633$ nm at the plasmon angle $\theta = \arcsin(n_{\text{eff}}/n_{\text{substrate}}) = 47^\circ$ (Bouhelier & Wiederrecht, 2005) deduced from Fig. 4. The propagation length L_{SPP} is directly deduced from the intensity distribution inside the waveguide measured by direct-plane leakage microscopy. Figure 6(a) shows a cross-sectional cut of the intensity measured along the waveguide. A semi-log graph (Fig. 6d) reveals the exponential nature of the attenuation. This attenuation originates from Joule losses into the metallic film during the mode propagation. The exponential regression gives $L_{\text{SPP}} = (4.1 \pm 0.1)$ μm in excellent agreement with the 4.08 μm numerically estimated using the differential method. The fit on experimental data extends for about 13 μ*m* corresponding to approximately three times the measured propagation length.

Because the previous section demonstrated a coupling of the QDs emission into the SPP mode, we can now investigate whether an optical gain is achievable by QDs-stimulated emission of SPP. To this aim, the QDs are optically pumped at $\lambda = 532$ nm, in addition to the direct excitation of the SPP at $\lambda = 633$ nm (Fig. 5). Figures 6(a–c) and their corresponding semi-log scale graphs (d–f) show a small variation of the propagation length as a function of pump irradiance. L_{SPP} increases from $L_{\text{SPP}} = (4.1 \pm 0.1)$ μm at null pump irradiance to $L_{\text{SPP}} = (5.3 \pm 0.1)$ μm at a pump irradiance of 600 W · cm^{-2}. Note that QDs photobleaching does not allow to increase the pump power above 600 W · cm^{-2}. Although rather low, the propagation length increase cannot be attributed to thermo-optical effects. Indeed, knowing the thermo-optical coefficient of the PMMA ($\partial n/\partial T = -1.05 \times 10^{-4}$ K^{-1}) we estimated that a L_{SPP} of 5.3 μm would correspond to a PMMA temperature around 530° C, far beyond the PMMA melting point (135° C). We therefore exclude this hypothesis to favour

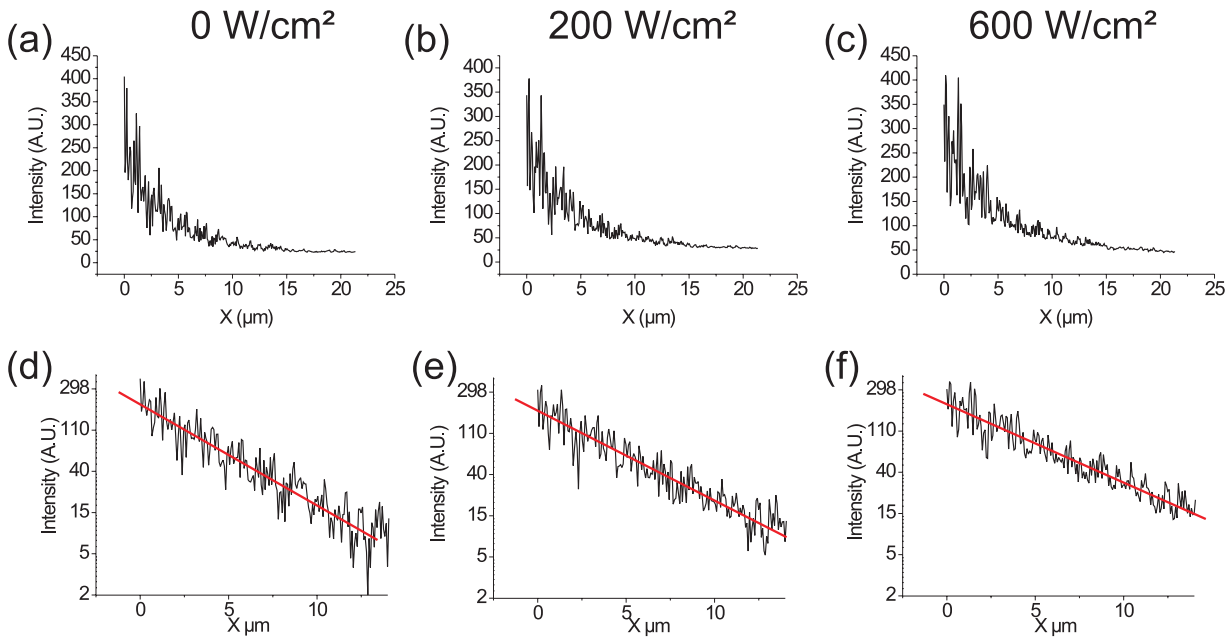

Fig. 6. Cross-sectional cut of the intensity measured along the DLSPPW in the image plane. A 532 nm laser of 0 $W \cdot cm^{-2}$ (a), 200 $W \cdot cm^{-2}$ (b) and 600 $W \cdot cm^{-2}$ (c) irradiance was used to optically pump the QDs in their excited states (see Fig. 5). (d–f) Same data in semi-logarithmic scale. Red lines are exponential fits.

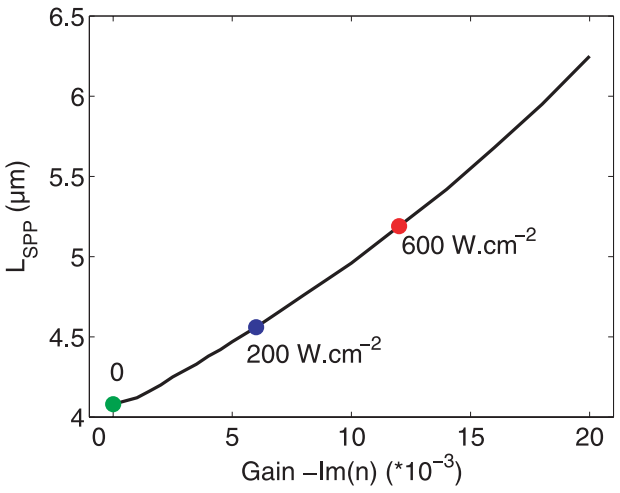

Fig. 7. The black line corresponds to the propagation length calculated when the imaginary part of the refractive index of the ridge varies from 0 to -10^{-2}. The measured propagation lengths are superimposed to the curve.

a partial compensation of the loss by stimulated emission of SPP (Grandidier *et al.*, 2009).

Figure 7 reports the calculated propagation length as a function of negative imaginary part of the polymer index. The black curve was obtained by using Green's dyad method (Colas des Francs *et al.*, 2009). This introduction of a negative imaginary optical index part mimics the effect of an optical gain on the propagation distance. The data points corresponds to the measured propagation distances for the three pump power used in the experiment. Finally, the increase of 30% of the propagation length obtained in confined plasmonic waveguides is comparable with recent experiments performed in extended planar film doped with dyes molecules (Seidel *et al.*, 2005; Noginov *et al.*, 2008).

Conclusion

We have shown that by combining leakage radiation microscopy with surface plasmon coupled emission, a complete characterization of the modes supported by an SPP waveguiding structure can be carried out. We applied the procedure to demonstrate partial loss compensation in an integrated plasmonic waveguide by a process analogous to an optical amplifier. We note that increasing the surface plasmon propagation distance by stimulated emission of SPP can also be achieved by electrically pumped semiconductors (Zhang *et al.*, 2004). The capability of limiting the shortcoming of metallic waveguides (losses) opens the door for realizing and integrating a surface plasmon laser (Bahriz *et al.*, 2006; Yu *et al.*, 2009).

Acknowledgements

The authors thank the European Commission (PLASMOCOM project, EC FP6 IST 034754 STREP) and the Regional Council of Burgundy for their financial support.

References

Bahriz, M., Moreau, V., Palomo, J. *et al.* (2006) Room-temperature operation of a $\lambda \approx 7.5$ μm surface-plasmon quantum cascade lasers. *Appl. Phys. Rev. Lett.* **90**, 027402 (4 pages).

Bergman, D.J. & Stockman, M.I. (2003) Surface plasmon amplification by stimulated emission of radiation: quantum generation of coherent surface plasmons in nanosystems. *Phys. Rev. Lett.* **90**, 027402.

Bouhelier, A. & Wiederrecht, G.P. (2005) Surface plasmon rainbow jet. *Opt. Lett.* **30**, 884–886.

Colas des Francs, G., Grandidier, J., Massenot, S., Bouhelier, A., Weeber, J. & Dereux, A. (2009) Integrated plasmonic waveguides: a mode solver based on density of states formulation. *Phys. Rev. B* **80**, 115419 (7 pages).

Drezet, A., Hohenau, A., Koller, D. *et al.* (2008) Leakage radiation microscopy of surface plasmon polaritons. *Mater. Sci. Eng. B* **149**, 220–229.

Enderlein, J. & Ruckstuhl, T. (2005) The efficiency of surface-plasmon coupled emission for sensitive fluorescence detection. *Opt. Exp.* **13**, 8855–8865.

Ebbesen, T., Genet, C. & Bozhevolnyi, S. (2008) Surface plasmon circuitry. *Phys. Today*. **61**, 44–50.

Grandidier, J., Massenot, S., Colas des Francs, G. *et al.* (2008) Dielectric-loaded surface plasmon polariton waveguides: figures of merit and mode characterization by image and Fourier plane leakage microscopy. *Phys. Rev. B* **78**, 245419 (9 pages).

Grandidier, J., Colas des Francs, G., Massenot, S., Bouhelier, A., Markey, L., Weeber, J., Finot, C. & Dereux, A. (2009) Gain assisted propagation in a plasmonic waveguide at telecom wavelength. *Nano Lett.* **9**, 2935–2939.

Gryczynski, I., Malicka, J., Gryczynski, Z. & Lakowicz, J.R. (2004) Surface plasmon-coupled emission with gold films. *J. Phys. Chem. B* **108**, 12568–12574.

Gryczynski, I., Malicka, J., Gryczynski, Z. & Lakowicz, J.R. (2005a) Radiative decay engineering. 4. Experimental studies of surface plasmon-coupled directional emission. *Anal. Biochem.* **324**, 170–182.

Gryczynski, I., Malicka, J., Jiang, W., Fischer, H., Chan, W.C., Gryczynski, Z., Grudzinski, W. & Lakowicz, J.R. (2005b) Surface plasmon-coupled emission of quantum dots. *J. Phys. Chem. B* **109**, 1088–1093.

Holmgaard, T. & Bozhevolnyi, S.I. (2007) Theoretical analysis of dielectric-loaded surface plasmon-polariton waveguides. *Phys. Rev. B* **75**, 245405 (12 pages).

Hoogenboom, J., Sanchez-Mosteiro, G., Colas des Francs, G., Heinis, D., Legay, G., Dereux, A. & van Hulst, N. (2009) The single molecule probe: nanoscale vectorial mapping of photonic mode density in a metal nanocavity. *Nano Lett.* **9**, 1189–1195.

Hunsperger, R.G. (2002) *Integrated Optics: Theory and Technology.* Springer, New York.

Krasavin, A.V. & Zayats, A.V. (2008) Three-dimensional numerical modeling of photonic integration with dielectric-loaded SPP waveguides. *Phys. Rev. B* **78**, 045425 (8 pages).

Massenot, S., Grandidier, J., Bouhelier, A., Colas des Francs, G., Weeber, J.-C., Markey, L. & Dereux, A. (2007) Polymer-metal waveguides characterization by Fourier plane leakage radiation microscopy. *Appl. Phys. Lett.* **91**, 243101 (3 pages).

Massenot, S., Weeber, J.-C., Bouhelier, A., Colas des Francs, G., Grandidier, J., Markey, L. & Dereux, A. (2008) Differential method for modelling dielectric-loaded surface plasmon polariton waveguides. *Opt. Exp.* **16**, 17599–17608.

Noginov, M.A., Zhu, G., Mayy, M., Ritzo, B.A., Noginova, N. & Podolskiy, V.A. (2008) Stimulated emission of surface plasmon polaritons. *Phys. Rev. Lett.* **101**, 226806.

Ozbay, E. (2006) Plasmonics: merging photonics and electronics at nanoscale dimensions. *Science* **311**, 189–193.

Seidel, J., Grafstrom, S. & Eng, L. (2005) Stimulated emission of surface plasmons at the interface between a silver film and an optically pumped dye solution. *Phys. Rev. Lett.* **94**, 177401 (4 pages).

Steinberger, B., Hohenau, A., Ditlbacher, H., Stepanov, A.L., Drezet, A., Aussenegg, F.R., Leitner, A. & Krenn, J.R. (2006) Dielectric stripes on gold as surface plasmon waveguides. *Appl. Phys. Lett.* **88**, 94104 (3 pages).

Yu, N., Wang, Q.J., Pügl, C. *et al.* (2009) Semiconductor lasers with integrated plasmonic polarizers. *Appl. Phys. Lett.* **94**, 151101 (3 pages).

Zhang, J., Gryczynski, Z. & Lakowicz, J.R. (2004) First observation of surface plasmon-coupled electrochemiluminescence. *Chem. Phys. Lett.* **393**, 483–487.

